

Transient Nonequilibrium Molecular Dynamic Simulations of Thermal Conductivity: 1. Simple Fluids¹

R. J. Hulse², R. L. Rowley^{2,3}, W. V. Wilding²

¹Paper presented at the Fifteenth Symposium on Thermophysical Properties, June 22-27, 2003, Boulder, Colorado, U.S.A

² Department of Chemical Engineering, Brigham Young University, Provo, Utah 84602, U.S.A.

³ To whom correspondence should be sent. E-mail: Rowley@byu.edu

Abstract

Thermal conductivity has been previously obtained from molecular dynamics (MD) simulations using either equilibrium (EMD) simulations (from Green-Kubo equations) or from steady-state nonequilibrium (NEMD) simulations. In the case of NEMD, either boundary-driven steady states are simulated or constrained equations of motion are used to obtain steady-state heat transfer rates. Like their experimental counterparts, these nonequilibrium steady-state methods are time consuming and may have convection problems. Here we report a new transient method developed to provide accurate thermal conductivity predictions from MD simulations.

In the proposed MD method, molecules that lie within a specified volume are instantaneously heated. The temperature decay of the system of molecules inside the heated volume is compared to the solution of the transient energy equation and the thermal diffusivity is regressed. Since the density of the fluid is set in the simulation only the isochoric heat capacity is needed in order to obtain the thermal conductivity. In this study the isochoric heat capacity is determined from energy fluctuations within the simulated fluid. The method is valid in the liquid, vapor and critical regions.

Simulated values for the thermal conductivity of a Lennard-Jones (LJ) fluid were obtained using this new method over a temperature range of 90–900 K and density range of 1-35 $\text{kmol}\cdot\text{m}^{-3}$. These values compare favorably with experimental values for Argon. The new method has an accuracy of $\pm 10\%$. Compared to other methods the algorithm is quick, easy to code, and applicable to small systems, making the simulations very efficient.

KEY WORDS: molecular dynamics; Lennard-Jones Fluid; nonequilibrium transient method; thermal conductivity

1. Introduction

Thermal conductivity is obtained from molecular dynamics using either equilibrium simulations [1-4] (from Green-Kubo equations) or from steady-state nonequilibrium simulations. [5-10] The Green-Kubo equations used to calculate thermal conductivity are,

$$\lambda = \frac{V}{T^2 \cdot k_b} \int_0^{\infty} \langle j_{\alpha}^{\varepsilon}(t) \cdot j_{\alpha}^{\varepsilon}(0) \rangle dt \quad (1)$$

$$\text{and } j_{\alpha}^{\varepsilon} = \frac{d}{dt} \left(\frac{1}{V} \sum_i r_{ci} \cdot (U_i - \langle U_i \rangle) \right) \quad (2)$$

where λ is thermal conductivity, V is volume, T is temperature, k_b is Boltzmann's constant, j_{α}^{ε} is heat flux, α is the component of the heat flux vector, t is time and U is internal energy. Equation 1 shows that the Green-Kubo relationship must be summed as time goes to infinity. The heat flux is a system property owing to the sum over all particles in equation 2, and therefore requires numerous evaluations of the correlation function in equation 1 to obtain reasonable statistical accuracy. The slow convergence of the integral in equation 1 is also problematic.

Steady-state NEMD simulations are also used to calculate thermal conductivity. One attempt is to specify the heat flux and use the simulation to find the temperature gradient. [5] The thermal conductivity is then obtained from Fourier's law. Like its experimental counterparts, this nonequilibrium steady-state method may have convection problems. Another method used to calculate thermal conductivity using nonequilibrium molecular

dynamics is the homogeneous field method. [8] In this method a constraint forces are introduced into the equation of motion to produce a desired heat flow and the thermal conductivity is then obtained from the force-flux relationship. However the applied field must be large to obtain a reasonable signal-to-noise ratio. Usually simulations at different heat fluxes must be performed and the thermal conductivity is obtained from an extrapolation to zero flux. As the magnitude of the applied field is decreased the computational time greatly increases. The NEMD methods avoid the long simulation times that result from the Green-Kubo relationship but they still suffer from the difficulty in determining the microscopic heat flux. The microscopic heat flux is an interparticle dynamic relationship. NEMD methods cannot easily be applied to systems that have long-range interactions because there are no available methods for calculating long-range dynamic interactions. [11]

2. Theory

The proposed method is a nonequilibrium transient method. The simulations are set up in a three dimensional box with periodic boundary conditions in all three directions. A random point in the simulation is selected and all molecules within a specified radius of that point are instantaneously heated by velocity rescaling. The volume element itself is treated as a “lumped capacitance” of uniform spatial temperature, and the kinetic energy of the molecules within the heated volume element is used to monitor its temperature decay. In this work, we have tracked the temperature decay until it is within 10% of the bulk temperature. This procedure of heating a small volume and recording the temperature-time

behavior for a short time is repeated many times to improve statistics for the temperature versus time curve. A short velocity rescale and a few equilibrium steps are used between each heating cycle. An average temperature-time trace can be generated from multiple simulations. Here we have repeated the temperatures jump until the average temperature decay is reasonably smooth as shown in Figure 1. The resultant temperature-time profile is compared to the solution of the transient energy equation, in a least squares sense, in order to obtain the thermal conductivity.

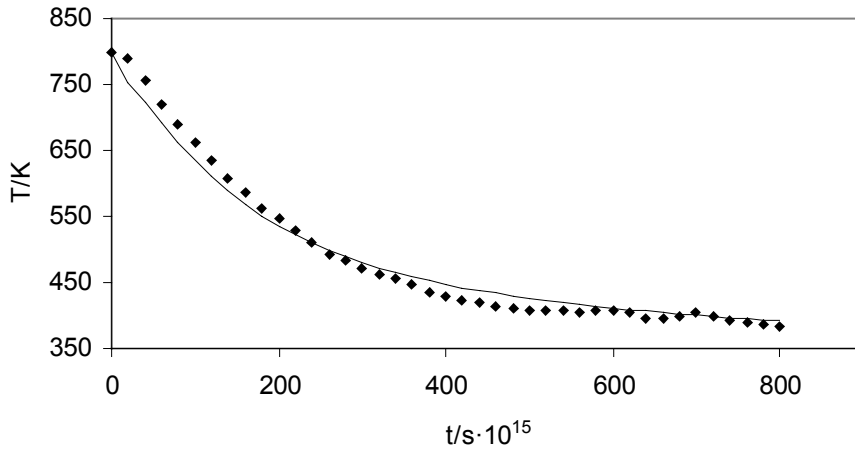


Figure 1: Typical transient temperature trace for $T = 350$ K and $\rho = 25$ kmol·m³ with a ΔT of 450 K showing the averaged simulation temperature (points) and the solution to equation 7 with regressed λ (line).

The transient energy equation balance may be written for a fixed volume element [12] as

$$\frac{\partial}{\partial t} \rho(U + \frac{1}{2}v^2) = -(\nabla \cdot \rho v(U + \frac{1}{2}v^2)) - (\nabla \cdot q) + \rho(v \cdot q) - (\nabla \cdot p v) - (\nabla \cdot [\tau \cdot v]) \quad (4)$$

where v is velocity, ρ is density, q is the heat flux, p is pressure and τ is the stress tensor. As is commonly done, the initial molecular momenta are normalized to eliminate any net momenta. While the artificial temperature jump could induce some net convective flow owing to any localized velocity within the selected volume element at the instant the velocities are rescaled to simulate the heating pulse. However, our simulations show that any such induced local molecular momentum is small and does not produce any directional bulk flow during the simulation of the temperature decay.

For the case of no bulk velocity, we can simplify equation 4 to

$$\frac{\partial}{\partial t}(\rho U) = -\nabla \cdot q = \frac{1}{r^2} \frac{\partial}{\partial r} \left(r^2 \lambda \frac{\partial T}{\partial r} \right), \quad (5)$$

where Fourier's law, applied to the spherically symmetric case of our heated volume element, has been used to obtain the second equality. Expansion of the time derivative on the left gives

$$\frac{\partial}{\partial t}(\rho U) = \rho c_v \frac{\partial T}{\partial t} + \rho \left(\frac{\partial U}{\partial V} \right)_T \frac{\partial V}{\partial t} + U \frac{\partial \rho}{\partial t} \quad (6)$$

where c_v is the constant volume heat capacity. We retain only the first term on the right

because $\frac{\partial \rho}{\partial t} = 0$ for $v = 0$ by the continuity equation and the volume does not change in

time. We thus obtain

$$\rho c_v \frac{\partial T}{\partial t} = \lambda \frac{1}{r^2} \frac{\partial}{\partial r} \left(r^2 \frac{\partial T}{\partial r} \right), \quad (7)$$

where we have also assumed that the thermal conductivity is independent of temperature. Although λ is a function of temperature, we can still use equation 7 by treating λ as an effective thermal conductivity for the particular temperature jump applied. However, the value of λ obtained may then depend upon the magnitude of the temperature jump employed.

Equation 7 can be solved for $T = T(t, \lambda)$ at the center of the heated volume by application of appropriate initial and boundary conditions. The initial condition is a step function in temperature between the bulk fluid temperature and that of the heated volume. We use a Neumann condition of zero flux at the center of the heated volume and a Dirichlet condition at a distance of $L/2$ from the heated center, where L is the simulation cell linear dimension. The best value of λ is obtained from a least-squares fit of the solution obtained from equation 7, $T = T(t, \lambda)$, to the transient temperature trace obtained from the simulation.

The regression of λ from equation 7 requires ρ and c_v . The density is fixed as an independent variable of the simulation but c_v may be determined from the simulation. The energy fluctuations in a canonical simulation using are related to c_v by

$$c_v = \frac{\langle U^2 \rangle - \langle U \rangle^2}{k_b \cdot T^2}. \quad (3)$$

Our procedure has been to first run the simulation in the canonical ensemble and calculate c_v from equation 3. The simulation is then changed to a microcanonical simulation and the previously discussed procedure of heating a small volume is followed. The simulated value of λ is then obtained by adjusting it to give the best match, in the least squares sense, of the simulated temperatures to equation 7.

The value of λ obtained from this procedure is actually the residual thermal conductivity, λ^r , because all of the potential energy terms in the simulation are relative to infinite molecular separation. For example, the potential energy is obtained from the sum of the pair potentials, which are zero at infinite separation. Likewise, the energy transfer in the simulated system is relative to the zero density of infinite volume fluid. Because we track the temperature of a heated volume element that at all time includes the same heated molecules, there would be no heat transfer from that volume element for a zero-density system because there would be no interactions between the heated molecules and the surrounding fluid and λ^r would be zero. The zero-density thermal conductivity, λ^0 , can be obtained from the well-known Chapmon-Enskog [13] solution of the Boltzmann equation:

$$\lambda^0 = 2.63 \cdot 10^{-23} \frac{\left(T/MW\right)^{3/2}}{\sigma^2 \cdot \Omega_V} \quad (8)$$

where λ^0 is in units of $\text{W} \cdot \text{m}^{-1} \cdot \text{K}^{-1}$, T is in units of K, MW is the molecular weight in $\text{kg} \cdot \text{mol}^{-1}$, σ is the characteristic dimension of the molecule in units of m, and Ω_V is a dimensionless collision integral. The actual thermal conductivity is then obtained from the

sum of the residual thermal conductivity obtained from the simulation and the zero-density Chapman-Enskog solution,

$$\lambda = \lambda^r + \lambda^0 . \quad (9)$$

3. Optimization of the Proposed Method

The efficiency of this transient simulation method depends upon three main: simulation size, size of the heated volume and the magnitude of the temperature jump. We have optimized each of these variables to give the best λ accurate per CPU time. The number of molecules (N) used in the simulation determines the simulation size. The size of the heated volume (V_H) is determined by the average number of molecules heated divided by the number density of the simulation.

The simulation size would ideally be small in order to minimize CPU time, but it must be large enough that the heated fraction of the simulated fluid is small. The heated volume also needs to be small so that the simulation size can be minimized, but it must contain sufficient molecules that the calculation of a temperature in the heated volume is meaningful. The magnitude of the temperature jump must be larger than the typical fluctuation of the temperature of a microcanonical simulation. The larger the temperature jump the shorter the simulation time due to the larger temperature decay obtained from a single simulation. If a small temperature jump is used then more simulations must be averaged in order to produce a smooth temperature decay.

The thermal conductivity of argon was simulated to optimize the parameters in this method. A central composite design experiment [14] was setup to optimize the simulation size, size of the heated volume and the magnitude of the temperature jump. These variables were optimized to give the most accurate thermal conductivity data in the liquid, vapor and critical regions. Table I gives the specific conditions at which the variables were optimized. Table I also shows the significant factors, the standard deviation of the thermal conductivity and the required number of integrations steps, which will be discussed later in the paper. The conditions at which the central composite design experiment was run are shown in Table II. The data obtained from the central composite design were fit to,

$$Y = A + B \cdot X_1 + C \cdot X_2 + D \cdot X_3 + E \cdot X_1 \cdot X_2 + F \cdot X_1 \cdot X_3 + G \cdot X_2 \cdot X_3 + H \cdot X_1^2 + I \cdot X_2^2 + J \cdot X_3^2 \quad (7)$$

where X_1 is the simulation size, X_2 is the heated volume, X_3 is the temperature jump and $A - J$ are regressed constants. The significant factors at the 95% confidence level that reduced the error between the simulated thermal conductivity and the thermal conductivity of argon correlated by Hanley [15] are given in Table I. The reason that there are no significant factors in the vapor region is that the reduced thermal conductivity obtained from the simulation is small compared to the zero-density portion of the reduced thermal conductivity, λ^0 . Both X_2 and X_2^2 would be significant in the vapor region if the confidence level was decreased to 90%. The regression showed that the heated volume must be minimized. When the heated volume is minimized the effect of the other

significant factors is also reduced. The factors were optimized to simultaneously minimize the error in all three regions.

Table I: Optimization Conditions and Results

Regions	T/K	$\rho/\text{kmol}\cdot\text{m}^3$	Significant Factors	$\lambda/\text{W}\cdot\text{m}^{-1}\cdot\text{K}^{-1}\cdot 10^3$ Average (Standard Deviation)	Integration Steps Required
Liquid	90	35	$X_2, X_1 \cdot X_2, X_2^2, X_2^2$	134.7 (4.70)	32000
Vapor	100	1	None	7.8 (0.225)	83000
Critical	350	30	X_2, X_3, X_3^2	107.1 (4.57)	69000

Table II: Central Composite Design

$N/\text{molecules}$	$V_H/\text{molecules}$	$\Delta T/\text{K}$
100	3	300
1000	3	300
100	3	1000
1000	3	1000
100	10	300
1000	10	300
100	10	1000
1000	10	1000
550	7	650
550	7	650
550	7	650
50	7	650
1328.5	7	650
550	7	44.5
550	7	1255.5
550	1	650
550	13	650
550	7	650
550	7	650
550	7	650

The optimized values for the simulation size, size of the heated volume and the magnitude of the temperature jump are 100 molecules, 3 molecules and 450 K, respectively. The

simulation size and heated volume allow for quick simulations. The optimized magnitude of the temperature jump allows for quick convergence but also results in an extremely large temperature gradient. The critical region is the only region in which the size of the temperature jump appears to be significant. Figure 2 shows the simulated thermal conductivity in the critical region for a range of temperature jumps. The regressed thermal conductivity is constant for temperature jumps below 650 K. The optimized temperature jump, 450 K, is well below this value. A large temperature jump may also cause velocity gradients. Which would invalidate equation 7. Because only a small number of molecules are heated, one would expect bulk velocities to form very slowly. The time that it takes for the temperature decay data to be recorded is significantly shorter than the time that it would take for a bulk velocity to form.

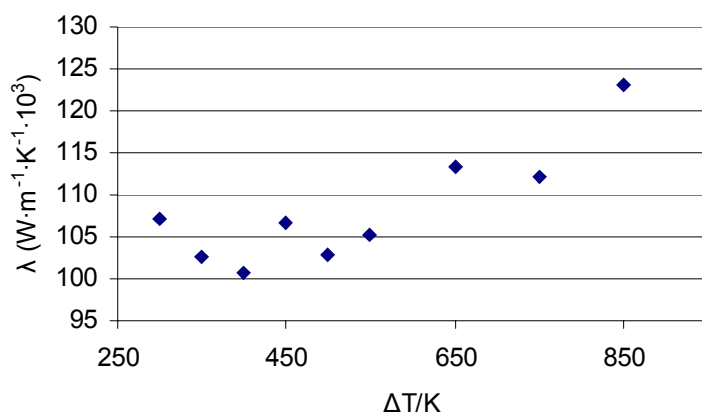


Figure 2: Dependence of the Thermal Conductivity on the Temperature jump in the Critical Region.

The precision of the new method was determined by running ten simulations all of which had different starting configurations at each of the conditions listed in Table I. The mean

and the standard deviation of the ten simulations are given in Table I. These standard deviations in the simulated thermal conductivity correspond to a confidence interval of $\pm 2.5\%$, $\pm 2.06\%$, and $\pm 3.05\%$ at the 95% confidence level for the liquid, vapor, and critical regions respectively. The last column in Table I shows the average number of integration time steps in the ten simulations that are required to simulate the thermal conductivity. As expected the number of integration steps increases as the density of the simulation decreases.

4. Results for Lennard-Jones Fluid

This new procedure was used to calculate the thermal conductivity of Lennard-Jones (LJ) fluid. The results using $\frac{\epsilon}{k_b} = 121.85$ K and $\sigma = 3.429$ angstroms for argon are given in Table III. The ideal gas (IG) values in Table III were predicted using equation 8. The shaded area is the two-phase region.

Table III: Simulated Thermal Conductivity of Argon in $\text{W}\cdot\text{m}^{-1}\cdot\text{K}^{-1}\cdot 10^3$

		T/K									
		90	95	100	150	250	350	450	600	750	900
$\rho/\text{kmol}\cdot\text{m}^{-3}$	IG	5.69	6.01	6.34	9.55	15.19	19.92	24.07	29.56	34.42	38.86
	1	7.1	7.4	7.8	11.0	16.8	21.5	26.0	31.5	37.0	41.9
	5				15.3	21.0	26.9	32.4	37.3	43.5	48.8
	10				26.7	31.1	33.9	41.1	48.8	53.1	55.8
	15				40.9	39.7	44.8	50.6	53.5	64.9	68.2
	20				43.5	52.3	58.9	62.1	72.5	79.9	83.7
	25	79.8	59.8	63.5	61.4	64.7	73.3	82.8	96.8	100.3	99.3
	30	90.0	86.6	84.6	95.4	102.7	107.8	112.7	122.5	130.5	119.3
	35	134.7	138.4	134.5	140.6	134.7	154.4	158.1	156.0	155.7	152.2

The error between the values in Table III and the correlation for argon proposed by Hanley [15] is shown in Table IV. The Hanley correlation is applicable only to 400 K. The largest error between the correlation and the simulated data is seen at 150 K and $10 \text{ kmol}\cdot\text{m}^{-3}$, which is in the critical region ($T_c = 150.86 \text{ K}$ and $\rho_c = 13.4 \text{ kmol}\cdot\text{m}^{-3}$) for argon. Near the critical point the correlation length of the fluid diverges. The size of the simulation cell must be twice the size of the correlation length to model the fluid accurately when using periodic boundary conditions. In order to maximize the efficiency of the simulation a small simulation cell was used. Our results in the critical region are expected to suffer from the inability to adequately simulate over the actual correlation length.

Table IV: Error Between Simulated LJ Thermal Conductivity and the Correlation Proposed by Hanley [15]

		T/K					
		90	95	100	150	250	350
$\rho/\text{kmol}\cdot\text{m}^{-3}$	IG	0%	0%	0%	0%	0%	0%
	1	5%	5%	1%	-2%	-3%	-3%
	5				17%	-1%	-7%
	10				33%	-12%	-6%
	15				16%	-2%	-2%
	20				9%	-1%	-2%
	25	-16%	12%	6%	7%	10%	10%
	30	4%	6%	7%	-6%	-1%	7%
	35	-6%	-10%	-8%	-14%	5%	4%

Experimental thermal conductivity data has been compiled for argon. [16,17] The simulated data points in Table III were interpolated to match the conditions of the experimental data. The error between the interpolated simulation data and the experimental

data is shown in Figure 3. As the density increases error in the simulated thermal conductivity goes from a positive to a negative bias. This is consistent with the fact the thermal conductivity in portions of the fluid is actually being sampled at a slightly higher temperature than the bulk temperature because of the temperature jump. Liquid thermal conductivity of argon decreases as the temperature increases and the vapor thermal conductivity increases with a temperature increase. These temperature trends are consistent with the S-shaped bias in the error.

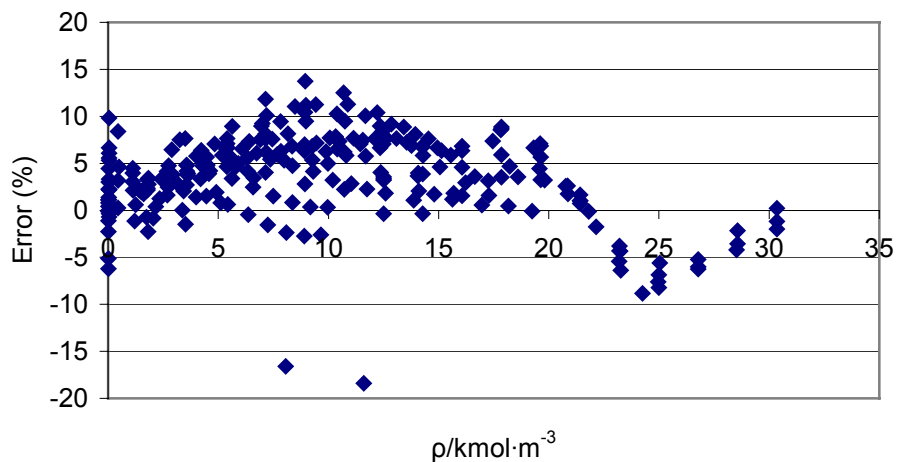


Figure 3: Error between Simulation and Experimental Data. [14, 15]

Previous researchers have simulated the thermal conductivity of argon using EMD and NEMD techniques. The results of previous researchers are given in Table V along with the results from this work. The values reported for this work have been interpolated from Table III. The data from the rapid transient method developed here compares favorably

with the correlated experimental data and is generally as good or better than that generated using other simulation methods

Table V: Comparison of Proposed Method to Previous Methods

T/K	$\rho/\text{kmol}\cdot\text{m}^{-3}$	$\lambda (\text{W}\cdot\text{m}^{-1}\cdot\text{K}^{-1}\cdot 10^3)$						This Work	Correlation [15]
		Volegsang [3] (EMD)	Paolini [7] (NEMD)	Heys [10] (NEMD)	Muller-Plathe [5] (NEMD)	Hohesisel [18] (EMD)			
85.30	35.01	-	-	-	139.6-121.2	143.9	129.10	131.0	
88.95	34.77	127.1	126.8	108.6	-	-	127.06	126.6	
114.54	29.44	94.2	-	70.8	-	-	84.77	86.2	
154.75	26.77	70	-	56.2	-	-	71.89	73.2	

5. Conclusions

A new transient method for calculating thermal conductivity from molecular dynamic simulations has been devised. The efficiency and simplicity of the method are strong advantages, allowing quick repeated simulations on small systems without the addition of added boundary conditions or modification to the equations of motion. The method has been benchmarked by comparison to previous simulation as well as correlated experimental argon thermal conductivity data. The simulated thermal conductivity values compare favorably with both previous simulations and the correlated values. The new method is able to predict thermal conductivity in the liquid, vapor and critical regions with the exception of near the critical point.

We assess error associated with this method as approximately $\pm 10\%$. The time that is required for the simulation depends upon the density of the simulation. A low density fluid take much longer to simulate then a high density fluid. The number of integration steps required, using a time step of when a $5 \cdot 10^{-15}$ s, to obtain a reasonably smooth average temperature decay is 32000, 69000, and 83000 at densities of 35, 30, and 1 $\text{kmol} \cdot \text{m}^{-3}$ respectively.

REFERNCES

1. D. M. Heyes, *J. Phys.: Condens. Matter* **6**, 6409 (1994).
2. R. K. Sharma, K. Tankeswar, and K. N. Pathak, *J. Phys.: Condens. Matter* **7**, 537 (1995).
3. R. Vogelsang, C. Hoheisel, and G. Ciccotti, *J. Chem. Phys.* **86**, 6371 (1987).
4. R. Vogelsang, G. Hoheisel, and M. Luckas, *Mol. Phys.* **64**, 1203 (1988).
5. F. Muller-Plathe, *J. Chem. Phys.* **106**, 6082 (1997).
6. T. Ikeshoji and B. Hafskjold, *Mol. Phys.* **81**, 251 (1994).
7. G. V. Paolini, G. Ciccotti, and C. Massobrio, *Phys. Rev. A* **34**, 1355 (1986).
8. D. J. Evans, *Phys. Lett. A* **91**, 457 (1982).
9. M. J. Gillian, *J. Phys. C* **16**, 869 (1983).
10. D. M. Heyes, *J. Chem. Soc. Faraday Trans.* **80**, 1363 (1984).
11. D. Bedrov and G. D. Smith, *J. Chem. Phys.* **113**, 8080 (2000).
12. R. B. Bird, W. E. Stewart, and E. N. Lightfoot, *Transport Phenomena* (John Wiley & Sons, New York, 1960)
13. B. E. Poling, J. M. Prausnitz, and J. P. O'Connell, *The Properties of Gases and Liquids* (McGraw-Hill, New York, 2001)
14. J. Lawson, J. Erjavec, *Modern Statistics for Engineering and Quality Improvement*

15. H. J. M. Hanley, R. D. McCarty, and W. M. Haynes, *J. Phys. Chem. Ref. Data* **3**, 979 (1974).
16. A. Michels, J. V. Sengers, and L. J. M. De Klundert, *Physica* **29**, 149 (1963).
17. B. Le Neindre, *Int. J. Heat Mass Transfer* **15**, 1 (1972).
18. C. Hoheisel, *Comput. Phys. Rep.* **12**, 29 (1990).